Azobenzene polymer surface deformation due to the gradient force of the optical near field of monodispersed polystyrene spheres

Taiji Ikawa,[1] Takuya Mitsuoka,[1] Makoto Hasegawa,[1] Masaaki Tsuchimori,[1] Osamu Watanabe,[1] and Yoshimasa Kawata[2]
[1]*Toyota Central R&D Labs. Inc., Nagakute, Aichi, 480-1192, Japan*
[2]*Faculty of Engineering, Shizuoka University, Johoku, Hamamatsu 432-8561, Japan*
(Received 25 June 2001; published 19 October 2001)

We report on the mechanism of azobenzene polymer surface deformation due to the optical near field around a dielectric sphere that is smaller than the wavelength of the incident light. We compared the deformation pattern on the surface with the calculated intensity distribution of the electric field around the sphere, and analyzed the polymer migration on the polymer surface using tapping-mode atomic force microscopy. This comparison and the polymer migration analysis show that the near-field gradient force induces the surface deformation.

DOI: 10.1103/PhysRevB.64.195408 PACS number(s): 78.66.Qn, 68.37.Uv

I. INTRODUCTION

The recent development of near-field optics and photonics opens a new door to spatially-control matter on a nanometer scale.[1] A variety of nanofabrication techniques employing optical near fields has been proposed.[1,2] In these circumstances, a working knowledge of the interaction between the optical near field and the surrounding material has become important[1,3] and is the subject of this research. Recently, our research group have demonstrated that topographical changes to the structure of individual monolayers of subwavelength-sized polystyrene spheres can be induced on the surface of an azobenzene derivative-containing polymer by exposure to a laser beam.[4–6] We have succeeded in transcribing a monolayer of 28 nm diameter spheres into a topographic image on an azobenzene polymer surface.[5] This result implies that the optical near field of spheres that are smaller than the wavelength of the incident light can cause surface deformation on the azobenzene polymer. (Hereafter we refer to spheres smaller than the wavelength of the light as Rayleigh spheres and spheres larger than the wavelength of the light as Mie spheres.) However, the mechanism of the surface deformation has not been clear up till now.

With regard to the surface deformation of azobenzene polymers, a topographic relief structure on an azobenzene polymer can be generated by exposure to an interference pattern from the coherent superposition of laser beams.[7–9] The topographic changes follow the intensity distribution of the electric field in the surface plane. This phenomenon has been considered to be a photodriven mass transport effect[7–9] and various driving forces behind it have been proposed, such as internal pressure,[7] light intensity gradients,[8] and intermolecular interaction.[9] However, neither the mass transport effect itself nor the nature of the driving force has been directly confirmed from the SRG experiments. In a previous paper, by studying the phase images created using tapping-mode atomic force microscopy (TMAFM),[6,10] we demonstrated that the viscoelastic properties of an azobenzene polymer surface treated with 100-nm diameter spheres change along with the topography. We concluded that this is definite evidence for the mass transport, while the driving force of the surface deformation has still been ambiguous.

In this article, we report that the three-dimensional gradient force of the optical near-field around a Rayleigh sphere brings about the surface deformation. First, we carried out scanning electron microscopy (SEM) to determine the position of the deformation relative to the sphere. The SEM image shows that the dents are formed just beneath the sphere. Secondly, we calculated the intensity distribution of the optical near field around the sphere, and compared its distribution with the surface deformation. The intensity distribution does not fully correspond with the surface deformation, but strongly suggests that the gradient force of the optical near field deforms the surface three-dimensionally. Thirdly, we performed TMAFM to analyze the mass transport on the azobenzene polymer surface. The mass transport evidences the surface deformation mechanism on the basis of the gradient force model.

II. EXPERIMENT

A urethane-urea copolymer containing donor-acceptor-substituted azobenzenes was synthesised and used as the substrate.[11] After dropping an aqueous solution of monodispersed polystyrene spheres onto the substrate, the water was evaporated from the solution. The spheres rearranged themselves via a self-organization process, and the sample was then irradiated with 488 nm wavelength coherent light from the Ar^+ laser. In order to rule out the influence of gravity on the deformation, all of the substrate surfaces were set aligned vertically during the exposures. Next the spheres were removed from the surface by immersing in water and/or by eluting in benzene, and then finally the surface was observed by field-emission SEM (JEOL, JSM-890) and TMAFM (Digital Instruments, Nanoscope IIIa).[6] A commercial silicon cantilever (Nanosensor, SSS NCH8, the tip radius of curvature was about 5 nm, the cantilever length was 125 μm, the force constant was 50 N/m, and the free resonant frequency was 298 kHz) was used for TMAFM. The scan speed was 500 nm/s in TMAFM. When the sample has steep and deep dents, imaging artifacts might arise from tip convolution effects.[12–14] To prevent the artifacts, FE-SEM images of the new tips chosen by random sampling were observed. Besides, the tip which could obtain the sharper images were selected and used for the AFM analysis.

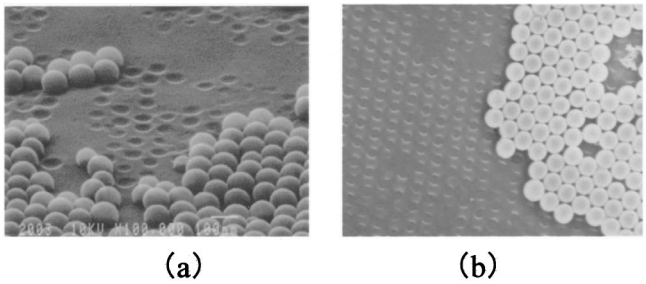

FIG. 1. SEM images of the substrate surface. These samples were treated by (a) 100 nm spheres (bird's eye view) and (b) 500 nm spheres (2D view). The samples were exposed to 488 nm and 0.5 W/cm^2 laser light.

The intensity distributions of the electric fields were calculated in a vacuum around both the 100 nm and 500 nm diameter polystyrene spheres using Mie's equation.[15,16] In the calculation, the refractive index of the polystyrene was taken to be 1.59, and the wavelength of incident light was 488 nm.

III. RESULTS AND DISCUSSION

The SEM images of the substrate surface with the 100 nm and 500 nm residual spheres are shown in Figs. 1(a) and 1(b), respectively. These images show that the dents are formed just under the spheres, regardless of the actual size of the spheres. In Fig. 1(a), the image clearly shows how the areas just under the spheres have been depressed while the surrounding area has been raised up. In addition, the spheres are embedded in the dents. In Fig. 1(b), the image shows that the dents and the residual spheres are arranged hexagonally. The spheres at the monolayer edge and the adjacent dents are aligned in a hexagonal arrangement; and therefore the spheres located themselves on the dent.

Also, we carried out AFM to analyze the surface shapes in detail. The sizes of the dents as a function of the exposed times are summarized in Fig. 2. The plots account for the dent formation processes practically. Figure 2(a) shows the change in the diameter of the dent with the exposed time. In the case of the 100 nm sphere, the diameter of the dent is as large as that of the corresponding sphere, and is almost unchanged during the exposure. In the case of the 500 nm sphere, the diameter of the dent is smaller than that of the corresponding spheres, and is slightly increased with the exposed time. Figure 2(b) shows the change in the depths of the dents. The depths of the dents induced by both the 100 nm and 500 nm spheres are increased with the exposed times, and are inclined to saturate. The saturated depths are about 50 nm and 150 nm for the 100 nm and 500 nm spheres, respectively. It should be emphasized that the diameters of the 100 nm sphere and the corresponding dent are about the same even in the early stage of the dent formation. (The contribution of the imaging artifacts originated from the tip convolution effect should be little because of the shallow dents.) The result represents that the surface deformation does not follow the shape of sphere; the shapes of the dent and the corresponding sphere are distinct from each other. The fact strongly suggests that some factors other than interfacial forces such as van der Waals forces play an important role for the surface deformation.

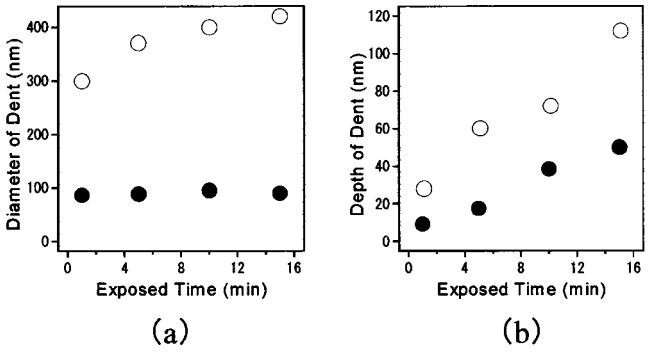

FIG. 2. Changes in the sizes of the dents during the exposure: (a) diameter; (b) depth. These samples were treated by the 100 nm spheres (●) and the 500 nm spheres (○). The samples were exposed to the 488 nm and 5 W/cm^2 laser light.

We examined the influence of the optical power on the dent formation, and confirmed that the surface deformation is essentially temperature independent. The samples with the 100 nm and 500 nm spheres were exposed to light with an optical power ranging from 0.01 W/cm^2 to 0.5 W/cm^2. The 0.01 W/cm^2 laser light caused a dent to form in the same manner as the 0.5 W/cm^2 laser light, with the total optical energies required being the same. During these exposures the polystyrene spheres, which had a glass transition temperature (T_g) of 105 °C, remained unchanged, so the temperature on the surface of the substrates should have been lower than 105 °C, which is well below T_g of the azobenzene polymer (145 °C). These results indicate that the contribution of the thermal effects to the surface deformation is low. Therefore, we conclude from these experiments that the surface deformation is optically induced.

Next, the calculated intensity distributions of the electric fields around the spheres are shown as the contour lines in Fig. 3, with the X-Z and Y-Z planes that contain the centers of the spheres. The intensity distributions change drastically with the sizes of the spheres. The electric fields around the 100 nm sphere, shown in Fig. 3(a), are enhanced at the sides of the spheres along the polarization directions of the incident light. The Rayleigh sphere hardly has any focusing effect on the incident light because of the diffraction limit, but works like an electric dipole. In contrast, the electric field around the 500 nm spheres, shown in Fig. 3(b), are enhanced towards the forward area of the sphere. The Mie sphere focuses the incident light because in this case the sphere works as a lens. These calculations reveal that the intensity distributions of the electric fields around the Rayleigh and Mie spheres are different. We believe that the calculated intensity distributions around the spheres in the vacuum are almost identical with the experimental system. We sometimes find that a solitary dent isolated from the rest of the arrangement can be formed on the surface [Fig. 1(a)]. The shapes of the isolated dents are about the same as those in the regular arrangement. We have tried to calculate the electric field around these isolated spheres on the polymer surface, and the

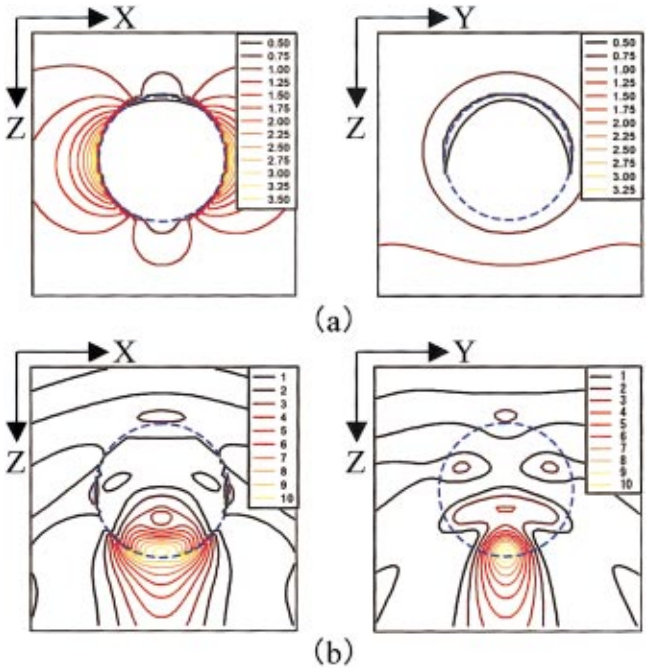

FIG. 3. (Color) Calculated intensity distributions of the electric fields around (a) the 100 nm spheres and (b) the 500 nm spheres. The left and right images show the X-Z and Y-Z planes. The direction of light propagation is along the Z direction, and is displayed from the top to the bottom of the images. The polarization directions are parallel to the X axis. The dotted circles represent the size of the spheres. The colored lines indicate the contour lines denoting the relative intensities to the incident light. The intensities are displayed in the legends.

complex refractive index of the polymer is taken into account in the calculation. The calculated distributions are qualitatively equivalent to those seen in the images in Fig. 3.

Comparing the experiments with the calculations, dent formation does not follow the intensity distribution of the electric field for the Rayleigh spheres, but it does for the Mie spheres. The Rayleigh sphere forms dents just below the sphere itself, while the intensity distribution in the surface plane is almost homogeneous. Therefore, it is necessary to take account of some factor acting on the surface besides the intensity distribution. In contrast, a Mie sphere causes a dent just below the sphere, which does obey the intensity distribution in the surface plane. In the cases where there is direct exposure to the interference pattern (SRG formation)[8] and to the focused Gaussian beam,[17] the deformation follows the intensity distribution of the electric fields in the surface plane. Since the Mie sphere acts like lens, as shown in Fig. 3(b), the dent induced by a Mie sphere is identical with one induced by direct exposure to a focused Gaussian laser beam.[17] These comparisons tell us that the surface deformation phenomenon originating from a Rayleigh sphere is a special case in that there is disagreement between the surface deformation and the intensity distribution in the surface plane. Some factor beyond the intensity distribution in the surface plane must be introduced in order to elucidate the phenomenon.

Regarding the azobenzene polymer surface deformation induced by the Rayleigh sphere, we propose that the mechanism originates from the three-dimensional near-field's gradient force. The proposed mechanism is outlined as follows. First, the azobenzene derivatives absorb the incident light, which induces trans-cis-trans isomerization.[18] Secondly, the isomerisation plasticizes the azobenzene polymer.[7,8,9] Thirdly, the gradient force of the electric field around the Rayleigh sphere attracts and draws up the azobenzene polymer. The direction of the gradient force is shown in Fig. 4. Concerning the gradient force, Ashkin first demonstrated the existence of the gradient force by conventional optics.[19] For the azobenzene polymer surface deformation, Kumar and coworkers presented a gradient force model that originated from the intensity distribution of the electric field in the surface plane.[8,17]

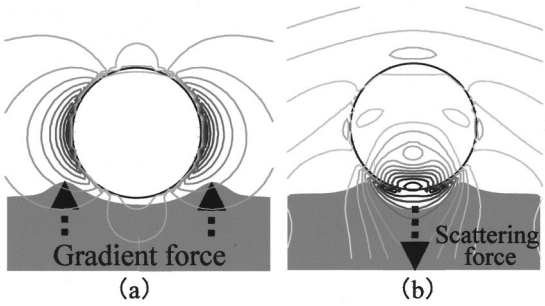

FIG. 4. Superposition of a cross section of the polymer surface and the calculated intensity distribution for (a) the 100 nm sphere and (b) the 500 nm sphere. The directions of the forces are represented in the images by the arrows.

The principle of the gradient force is described as follows.

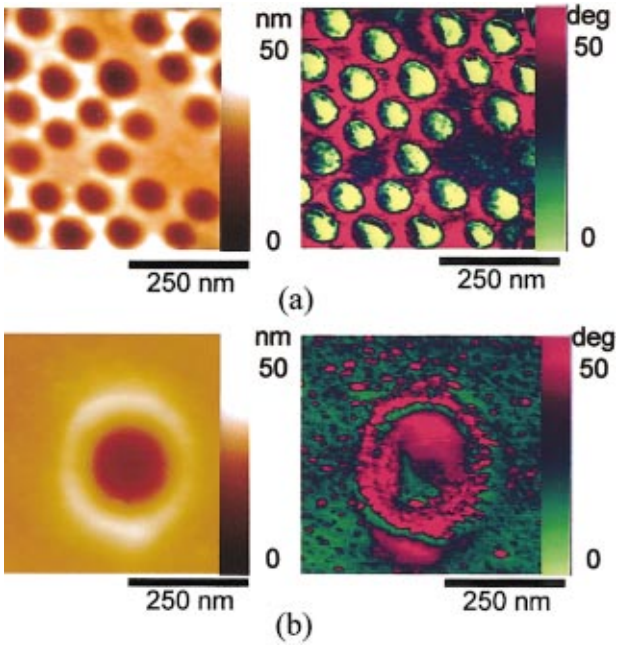

FIG. 5. (Color) TMAFM images of the substrate surface. These samples were treated by (a) the 100 nm spheres and (b) the 500 nm spheres. The left-hand and right-hand images show the topographic and phase images, respectively. All of the samples were irradiated with 488 nm laser light at 0.01 W/cm^2 for 250 min.

Dielectric materials in a vacuum are affected by the optical electromagnetic field $\mathbf{E}=\mathbf{E}_0\exp(i\omega t)$ and $\mathbf{H}$, so that the dielectric materials receive a dynamic force $\mathbf{f}_d$:

$$\mathbf{f}_d=\varepsilon_0\chi\left\{\nabla\left(\frac{1}{2}\mathbf{E}^2\right)+\frac{1}{\varepsilon_0}\frac{\partial\mathbf{p}_e}{\partial t}\right\}, \tag{1}$$

where ε_0 is the electric permittivity, χ is the electric susceptibility of the dielectric material, and $\mathbf{p}_e=\varepsilon_0\mathbf{E}\times\mathbf{B}$ is the momentum of light. Dielectric materials that absorb light are often represented phenomenologically by a complex susceptibility,

$$\chi=\chi'-i\chi'', \tag{2}$$

corresponding to a complex permittivity $\varepsilon=\varepsilon_0(1+\chi)$. Substituting Eq. (2) into Eq. (1) and extracting only the real part of Eq. (1), we obtain an equation relating to the dynamic force,

$$\mathbf{f}_d=\varepsilon_0\chi'\left\{\nabla\left(\frac{1}{2}\mathbf{E}^2\right)\right\}+2\pi f\chi''\mathbf{p}_e, \tag{3}$$

where $2\pi f=\omega$. In Eq. (3), the first and second terms are related to the gradient of the intensity of the electric field and the absorption of the dielectric material, respectively.

The directions of these forces are dependent on χ. We obtain $\chi'=1.87$ and $\chi''=1.10$ for the isotropic azobenzene polymer at 488 nm wavelength. These data are calculated from the refractive index and the extinction coefficients measured by spectro-ellipsometry.[20] Therefore, the gradient force [the first term in Eq. (3)] attracts the azobenzene polymer from the region with the weaker electric field towards the stronger field. On the other hand, the force induced by absorption [the scattering force, the second term in Eq. (3)] acts parallel with the momentum of the photon.

We simply estimated the gradient forces and the scattering forces around the spheres from Eq. (3) and the distributions shown in Figs. 3. We confirmed that the gradient force is larger than the scattering force in the case of the Rayleigh sphere. Thus the gradient force around the Rayleigh sphere draws up the azobenzene polymer around the sides of the spheres [Fig. 4(a)], such that a dent is formed on the surface. Oppositely, the scattering force is dominant in the case of the Mie sphere. Hence, the scattering force pushes the azobenzene polymer chain into the substrate [Fig. 4(b)]. In addition to these optically induced forces, the interfacial forces such as the van der Waals forces might play some part for the surface deformation. However, the surface deformation does not follow the shape of the dent as shown in Fig. 2 and Fig. 4. The contribution of the optically induced forces is more remarkable than the interfacial forces.

The direction of the polymer migration was confirmed by TMAFM. The phase image during TMAFM provides a map of stiffness variations on the surface such that a stiffer region displays a more positive phase shift.[6,10] The reason for this is that the phase shift $\Delta\Phi_0$ is approximately described as

$$\Delta\Phi_0\propto\sqrt{\langle A\rangle}E^*(Q/k), \tag{4}$$

where $\langle A\rangle$ is the time-averaged value of the contact area, E^* is the effective modulus, Q is the quality factor of a cantilever, and k is the spring constant of the cantilever. E^* is proportional to the stiffness when the tip is much harder than the sample. In our experiments, $\langle A\rangle$ is a constant, since we operated the TMAFM at room temperature and at moderate tapping setting (large A_0 and somewhat small r_{sp}). Accordingly, we determined that the phase shift is dominated by the stiffness on the surface, such that a stiffer region has a greater phase shift. The stiffness variation on the surface represents polymer migration because the area condensed by the migration becomes harder.

The TMAFM images of the surface treated by the 100 nm spheres are shown in Fig. 5(a). The phase image shows that the insides of the dents become relatively softer (smaller phase shift) and the vicinal area becomes harder (larger phase shift). This result accounts for the polymer migration induced by the gradient force. If the gradient force of the optical near-field draws up and gathers the azobenzene polymer chain to the sides of the sphere [Fig. 4(a)], the margin and the inside of the dent become harder and softer, respectively. The stiffness variation on the surfaces analyzed by TMAFM evidences the proposed mechanism on the basis of the optical near-field's gradient force.

The TMAFM images of the surface treated by the 500 nm spheres is displayed in Fig. 5(b). In contrast to Fig. 5(a), the phase image shows that the insides of the dents become relatively harder (larger phase shift). This result is consistent with our proposed theory that the polymer chain is pushed into the inside of the substrate due to the scattering force. Furthermore, if the refractive index of the azobenzene polymer changes with the intensity distribution of the electric field during the exposure, the χ' component in the plane of the surface might become apparently negative, as Kumar and co-workers pointed out. The azobenzene polymer chains move from stronger electric field areas to the weaker areas in the surface plane due to the gradient force in the surface plane. Thus the inside of the dent becomes harder.

IV. CONCLUSION

We have proposed calculations and experiments to explain the surface deformation of an azobenzene polymer that is induced by the exposure to light of spheres of 100 nm and 500 nm diameter. The calculated intensity distributions around the 100 nm and 500 nm spheres are distinct from one another, and disagree with the observed deformation in the cases of the 100 nm spheres. From this data, a mechansim based on the optical near-field's gradient force is proposed. Analysis by TMAFM of the polymer migration on the surface strongly supports the proposed mechanism.

[1] M. Ohtsu and H. Hori, *Near-Field Nano-optics* (Kluwer Academic, New York, 1999).
[2] E. Betzig, J. K. Trautman, R. Wolfe, E. M. Gyorgy, P. L. Finn, M. H. Kyrder, and C. H. Chang, Appl. Phys. Lett. **61**, 142 (1992); J. Tominaga, T. Nakano, and N. Atoda, *ibid.*, **73**, 2078 (1998).
[3] R. C. Dunn, Chem. Rev. **99**, 289 (1999).
[4] Y. Kawata, C. Egami, O. Nakamura, O. Sugihara, N. Okamoto, M. Tsuchimori, and O. Watanabe, Opt. Commun. **161**, 6 (1999).
[5] O. Watanabe, T. Ikawa, M. Hasegawa, M. Tsuchimori, Y. Kawata, C. Egami, O. Sugihara, and N. Okamoto, Mol. Cryst. and Liq. Cryst. Sci. Technol., Sect. A **345**, 305 (2000).
[6] T. Ikawa, T. Mitsuoka, M. Hasegawa, M. Tsuchimori, O. Watanabe, Y. Kawata, C. Egami, O. Sugihara, and N. Okamoto, J. Phys. Chem. B **104**, 9055 (2000).
[7] P. Rochon, E. Batalla, and A. Natansohn, Appl. Phys. Lett. **66**, 136 (1995).
[8] J. Kumar, L. Li, X. L. Jiang, D. Y. Kim, T. S. Lee, and S. Tripathy, Appl. Phys. Lett. **72**, 2096 (1998).
[9] T. G. Pedersen, P. M. Johansen, N. C. R. Holme, P. S. Ramanujam, and S. Hvilsted, Phys. Rev. Lett. **80**, 89 (1998).
[10] S. N. Magonov, V. Elings, and M.-H. Whangbo, Surf. Sci. **375**, L385 (1997).
[11] O. Watanabe, M. Tsuchimori, and A. Okada, J. Mater. Chem. **6**, 1487 (1997).
[12] D. J. Keller and F. S. Franke, Surf. Sci. **294**, 409 (1993).
[13] D. Keller, Surf. Sci. **253**, 353 (1991).
[14] L. Montelius and J. O. Tegenfeldt, Appl. Phys. Lett. **62**, 2628 (1993).
[15] G. Mie, Ann. Phys. (Leipzig) **25**, 377 (1908).
[16] M. Born and E. Wolf, *Principles of Optics*, 5th ed. (Pergamon, Oxford, UK, 1975), Chap. 13.
[17] S. Bian, L. Li, J. Kumar, D. Y. Kim, J. Williams, and S. K. Tripathy, J. Appl. Phys. **86**, 4498 (1999).
[18] H. Rau, *Photochemistry and Photophysics, Vol. II* (CRC Press, Boca Raton, FL, 1990), pp. 119–142.
[19] A. Ashkin, J. M. Dziedzic, J. E. Bjorkholm, and S. Chu, Opt. Lett. **11**, 288 (1986).
[20] O. Watanabe and M. Tsuchimori, Polymer **42**, 6447 (2001).